PHYSICAL REVIEW A VOLUME 34, NUMBER 3 SEPTEMBER 1986

Projectile-ionization cross sections for H-like ions in collisions with N_2, O_2, Ne, and Ar targets

Toshiaki Kaneko
Department of Applied Physics, Okayama University of Science, Ridai-cho 1-1 Okayama 700, Japan
(Received 17 March 1986)

Electron-loss cross sections for hydrogenlike ions with atomic number Z_1 ($2 \le Z_1 \le 7$) and with velocity v ($0.3v_0 \lesssim v/Z_1 \lesssim 6v_0$; v_0 is the Bohr velocity) are investigated in collisions with N_2, O_2, Ne, and Ar targets using the unitarized impact-parameter method. In order to describe the form factors of these targets, we use the modified Molière electron distributions where the parameters appearing in the Molière potential are slightly modified to fit the form factors obtained from Hartree-Fock wave functions in the small momentum-transfer region. Then we find the electron-loss cross sections sensitive to those parameters at high velocities. The scaling relations, characterized by the reduced cross section $\tilde{\sigma}$ ($=Z_1^m\sigma$) versus the reduced velocity $\tilde{v}$ ($=v/Z_1$), are presented, where $m=2.8$ for N_2 and O_2, 2.6 for Ne, and 2.4 for Ar. Here the molecular effect in N_2 and O_2 targets and the polarization of target electron clouds due to a projectile are both neglected. These scalings yield good agreement with the reported data, particularly when $\tilde{v} \lesssim 1$.

I. INTRODUCTION

Charge states of energetic ions passing through matter have been an important problem in studies of ion-beam–material interactions and plasma-wall interactions, etc., in order to investigate both target- and projectile-excitation processes and related phenomena. For example, energy loss and energy straggling of incident ions depend on the net charge[1–6] and, if the ions are partially stripped, also depend on the spatial electron distribution of the bound electrons in them.[7,8] Recently, stopping powers, energy stragglings, and the charge-fluctuation contribution to energy straggling have been studied for ion beams with several charge states allowed in matter, where the size effect of partially stripped ions and the charge fractions are included.[9,10]

In principle, charge states of impinging ions are determined by the cross sections for charge-changing processes, i.e., electron capture from a target and electron loss of a moving particle.[11] As for the study of the electron-loss process, several theories are available so far. When we consider the cases where the interaction Hamiltonian is sufficiently small and the projectile velocity is sufficiently large compared with the orbital velocity of the excited electron, the first Born approximation (FBA) can be successfully applied to the investigation of electron-loss and -excitation processes. Particularly, in plasmaphysics and astrophysics the FBA has been often used with success in studying such processes for impurity ions and light ions colliding with H and He targets.[12–14] There the widely used closure expression and a scaling law for electron loss are available. However, the FBA breaks down for ions colliding with heavy target atoms especially around the velocity $v \sim Z_1 v_0$ (Z_1 is the atomic number of a projectile) where the electron-loss cross section becomes maximum and the FBA theory usually yields larger cross sections. On the other hand, based on the free collision approximation, Bohr[15] presented the formula for an electron-loss cross section for an ion with velocity v colliding with a heavy target atom with atomic number Z_2, where the cross section is proportional to $Z_2^{2/3}$ and v^{-1} for $v \gg v_b$ (v_b is the orbital velocity of the ejected electron). In spite of its simple form, this result is at least in qualitative agreement with data. Bohr's formula shows a velocity dependence different from the asymptotic velocity dependence of the FBA theory.

In order to improve the FBA especially around $v \sim Z_1 v_0$ for high-Z_2 targets and to obtain more satisfactory agreement over a wider velocity range than the Bohr formula, the unitarized impact-parameter method is used.[16] This method includes interaction matrix elements to infinite order under some approximations, as will be mentioned in the text. According to this theory, the electron-loss and -excitation cross sections for a He^+ ion are found to depend only weakly on Z_2 in the regime $Z_2 \gtrsim 10$ at the velocities considered. In addition, the energy dependences of the electron-loss cross sections for several gaseous targets are in good agreement with the reported data over wide impact-energy ranges.

The aim of this paper is to investigate the electron-loss process for hydrogenlike ions both with Z_1 ranging from 2 to 7 and v ($0.3v_0 \lesssim v/Z_1 \lesssim 6v_0$) as a direct extension of Ref. 16. Furthermore, scaling relations in the electron-loss cross section are proposed, which are different from the FBA prediction. In Sec. II our procedure is briefly reviewed, and in Sec. III numerical results and discussion are presented. We use atomic units throughout this paper unless otherwise stated.

II. PROCEDURE

Since the theoretical background has been given previously,[16] only a brief description is presented. We assume that a projectile with velocity v moves along a straight-line trajectory with impact parameter b. Here a projectile is hydrogenlike and, therefore, has only one electron, while a target atom is allowed to have many electrons. We treat the motion of a projectile classically and that of electrons quantum mechanically. The interaction Hamiltonian of our system is written as

$$V_{\rm int}(t) = -Z_2/|\mathbf{R}+\mathbf{r}_1| + \sum_j (-Z_1/|\mathbf{R}-\mathbf{r}_{2j}| + 1/|\mathbf{r}_1-\mathbf{r}_{2j}+\mathbf{R}|) , \qquad (2.1)$$

where the position vectors $\mathbf{r}_1$, $\mathbf{r}_{2j}$ $(j=1,2,\ldots,Z_2)$, and $\mathbf{R}$ refer to a projectile's electron, target electrons, and a projectile nucleus relative to nucleus of a target atom. The time dependence of $V_{\rm int}(t)$ is introduced through $\mathbf{R}=\mathbf{b}+\mathbf{v}t$. In obtaining the transition amplitudes to final states, the following approximations are adopted: (1) drop the chronological ordering operator in evaluating the time-ordered multiple integrals of the interaction Hamiltonian and (2) fix either the bra or the ket vector to the ground-state bra or ket vector of each matrix element of the interaction Hamiltonian in any order terms.

Under the above conditions, the transition probability $\mathcal{P}_{nk}(b)$ for the process that both a target atom and a projectile are excited to the excited state k of the atom and n of the projectile ($|n;k\rangle$), respectively, from the ground states denoted by 0 ($|0;0\rangle$) is obtained[17] as

$$\mathcal{P}_{nk}(b) = [P_{nk}(b)/P_t(b)]\sin^2[P_t(b)^{1/2}] , \qquad (2.2)$$

and the survival probability $\mathcal{P}_{00}(b)$ of the ground state is

$$\mathcal{P}_{00}(b) = \cos^2[P_t(b)^{1/2}] , \qquad (2.3)$$

where

$$P_t(b) = \sum_{n,k} P_{nk}(b) , \quad P_{nk}(b) = \left| \int_{-\infty}^{\infty} dt \langle n;k \,|\, \tilde{V}(t) \,|\, 0;0\rangle \right|^2 . \qquad (2.4)$$

The operator $\tilde{V}(t)$ has vanishing diagonal matrix elements because it is derived from the interaction Hamiltonian $V_{\rm int}(t)$ in (2.1) by means of a unitary transformation of subtracting its diagonal part $V_{{\rm int},d}(t)$ from $V_{\rm int}(t)$ itself. The explicit form is

$$\tilde{V}(t) = \exp[i\gamma(t)][V_{\rm int}(t) - V_{{\rm int},d}(t)]\exp[-i\gamma(t)] \qquad (2.5)$$

and the matrix elements of $\gamma(t)$ are given as

$$\langle n;k \,|\, \gamma(t) \,|\, n';k'\rangle = \left[\int_{\infty}^{t} dt' \langle n;k \,|\, V_{\rm int}(t') \,|\, n;k\rangle + \varepsilon_{nk} t \right] \delta_{nn'}\delta_{kk'} , \qquad (2.6)$$

where ε_{nk} denotes the energy of the state $|n;k\rangle$. The matrix element $\langle n;k \,|\, V_{\rm int}(t') \,|\, n;k\rangle$ is composed of three energy-level-shift terms at the position $\mathbf{R}(t')$: two of them are the level shift of a projectile state n due to both a target nucleus and the electron distribution of a target state k, and the last term is that of a target state k due to a projectile nucleus. These terms become important at lower impact velocities. Later, we restrict ourselves to the velocity range $v \gtrsim 0.6 v_0$ so that these are all neglected. This is the third approximation for us.

As is understood immediately from (2.4), the projectile-ionization and -excitation probabilities are contributed both from the target-inelastic ($k \neq 0$) and from the target-elastic ($k=0$) processes. Instead of estimating directly the quantities $P_{n0}(b)$ and $P_{nk}(b)$ in (2.4), let us consider the integrals of them over b:

$$\sigma_{\rm el} = \int_0^{\infty} db\, 2\pi b P_{n0}(b) , \quad \sigma_{\rm inel} = \sum_{k(\neq 0)} \int_0^{\infty} db\, 2\pi b P_{nk}(b) , \qquad (2.7)$$

where $\sigma_{\rm el}$ and $\sigma_{\rm inel}$ are equal to the cross sections within the framework of the FBA, and therefore, they are roughly proportional to Z_2^2 and Z_2, respectively. This relation obtained from the FBA is expected to be valid in the relation between $P_{n0}(b)$ and $P_{nk}(b)$ themselves. It can be concluded, therefore, that $P_{n0}(b)$ is more dominant than $\sum_{k(\neq 0)} P_{nk}(b)$. According to this consideration, all $P_{nk}(b)$'s ($k \neq 0$) can be neglected as long as heavy (high-Z_2) target atoms are treated. Thus we neglect the target-inelastic contribution to the electron-loss cross section in comparison with the target-elastic one. This is the fourth approximation for us.

At this stage, the projectile-ionization is contributed only from the target-elastic process, in other words, it is caused by the average potential field provided by a target atom. Here this average potential is approximately described by the Molière potential

$$V_M(\mathbf{r}) = -(Z_2/r) \sum_{i=1}^{3} \alpha_i \exp(-\beta_i r/a_{\rm TF}) , \quad a_{\rm TF} = 0.8853 Z_3^{-1/3} , \qquad (2.8)$$

where the parameters are given by $(\alpha_1,\alpha_2,\alpha_3) = (0.10, 0.55, 0.35)$ and $(\beta_1,\beta_2,\beta_3) = (6.0, 1.20, 0.30)$, and $a_{\rm TF}$ is the Thomas-Fermi (TF) screening length. Using Poisson's equation, the spatial electron distribution $\rho(\mathbf{r})$ in an atom is immediately obtained. By applying the Fourier transform to $\rho(\mathbf{r})$, the elastic form factor $\rho(\mathbf{q})$ can be found in the form

$$\rho(\mathbf{q}) = Z_2 \sum_{i=1}^{3} \alpha_i / [1 + (a_{\rm TF} q/\beta_i)^2] . \qquad (2.9)$$

The Molière potential $V_M(r)$ has the following Fourier component:

$$V_M(\mathbf{q}) = -(4\pi/q^2)[Z_2 - \rho(\mathbf{q})] . \qquad (2.10)$$

This term actually appears in $P_{n0}(b)$, as will be seen later.

To classify projectile-ionization and -excitation processes, the subscript of $P_{n0}(b)$ is changed to $P_{\rm ion}(b)$ for ionization, and $P_{{\rm exc},n}(b)$ for excitations to the nth state. The initial wave function is the hydrogenic 1s wave function for both processes:

$$\phi_0(\mathbf{r}) = (\pi a_1^3)^{-1/2} \exp(-r/a) , \quad a_1 = Z_1^{-1} . \qquad (2.11)$$

The final-state wave function for ionization is assumed to be a plane wave for simplicity with a wave vector $\boldsymbol{\kappa}$:

$$\phi_\kappa(\mathbf{r})=(2\pi)^{-3/2}\exp(i\boldsymbol{\kappa}\cdot\mathbf{r}) . \tag{2.12}$$

Using the above wave functions and integrating the square of the absolute value of the transition matrix element over the wave vector $\boldsymbol{\kappa}$, the expression of $P_{\text{ion}}(b)$ is obtained. In order to investigate a scaling problem in the electron-loss cross section, the formula is written in the following reduced form:

$$P_{\text{ion}}(\tilde{b})=\frac{2^6Z_2^2}{\pi(Z_1\tilde{v})^2}\int_0^\infty d\tilde{\kappa}_y\tilde{\kappa}_y\int_{-\infty}^{\infty}d\tilde{\kappa}_z\sum_{m=0}^{\infty}h_m\left|\int_0^\infty d\tilde{q}_y\tilde{q}_yJ_m(\tilde{q}_y\tilde{b})\tilde{q}^{-2}\times[Z_2-\rho(\tilde{q})]\left[\frac{(\tilde{A}^2-\tilde{B}^2)^{1/2}-\tilde{A}}{\tilde{B}}\right]^m\left[\frac{\tilde{A}}{(\tilde{A}^2-\tilde{B}^2)^{3/2}}+\frac{m}{(\tilde{A}^2-\tilde{B}^2)}\right]\right|^2 , \tag{2.13}$$

where

$$\begin{aligned}&\tilde{q}=(\tilde{q}_y^2+\tilde{q}_z^2)^{1/2},\quad \tilde{q}_z=-(\varepsilon_\kappa^{(p)}-\varepsilon_1^{(p)})/\tilde{v},\quad \varepsilon_\kappa^{(p)}=\tfrac{1}{2}(\tilde{\kappa}_y^2+\tilde{\kappa}_z^2) ,\\ &\varepsilon_1^{(p)}=-\tfrac{1}{2},\quad \tilde{A}=1+\tilde{q}_y^2+\tilde{\kappa}_y^2+(\tilde{q}_z-\tilde{\kappa}_z)^2,\quad \tilde{B}=2\tilde{q}_y\tilde{\kappa}_y .\end{aligned} \tag{2.14}$$

In (2.13), $J_m(\tilde{q}_y\tilde{b})$ denotes the Bessel function of mth order, and $h_m=1$ for $m=0$ and 2 for m a positive integer. The subscripts z and y in (2.13) and (2.14) indicate the direction of motion of a projectile and the direction perpendicular to the z direction, respectively. Moreover, the reduced velocity $\tilde{v}$, the reduced impact parameter $\tilde{b}$, and the reduced Thomas-Fermi screening length $\tilde{a}_{\text{TF}}$ are, respectively, defined by

$$\tilde{v}=v/Z_1,\quad \tilde{b}=Z_1b,\quad \text{and}\ \tilde{a}_{\text{TF}}=Z_1a_{\text{TF}} . \tag{2.15}$$

On the other hand, when we calculate the excitation matrix element for a transition to $|\,n,n_1,n_2\rangle$ from $|1,0,0\rangle$ in the parabolic coordinate system, $P_{\text{exc},n}(\tilde{b})$ has the following form:

$$P_{\text{exc},n}(\tilde{b})=\frac{4Z_2^2}{Z_1^2\tilde{v}^2}\sum_{n_1\ (\text{or}\ n_2)}^{n-1}\left|\int_0^\infty d\tilde{q}_y\tilde{q}_yJ_0(\tilde{q}_y\tilde{b})\tilde{q}^{-2}[Z_2-\rho(\tilde{q})]\langle n,n_1,n_2\,|\exp(i\tilde{\mathbf{q}}\cdot\mathbf{r})\,|\,1,0,0\rangle\right|^2 , \tag{2.16}$$

with

$$\langle n,n_1,n_2\,|\exp(i\tilde{\mathbf{q}}\cdot\mathbf{r})\,|\,1,0,0\rangle =2^4n^3\tilde{q}[n\tilde{q}-i(n_1-n_2)][(n^2-1)+n^2\tilde{q}^2-i2n\tilde{q}]^{n_1-1}[(n^2-1)+n^2\tilde{q}^2+i2n\tilde{q}]^{n_2-1}/[(n+1)^2+n^2\tilde{q}^2]^n , \tag{2.17}$$

where

$$\begin{aligned}&\tilde{q}=(\tilde{q}_y^2+\tilde{q}_z'^2)^{1/2} ,\\ &\tilde{q}_z'=-(\varepsilon_n^{(p)}-\varepsilon_1^{(p)})/\tilde{v} ,\\ &\varepsilon_n^{(p)}=-(\tfrac{1}{2})n^{-2}\quad (n=2,3,\dots) .\end{aligned} \tag{2.18}$$

In the above equations, n is a principal quantum number, and other quantum numbers n_1 and n_2 (n_1 or $n_2=0,1,2,\dots,n-1$) are related to n through the equation $n_1+n_2+1=n$. The energy level of a state n of the projectile is denoted by $\varepsilon_n^{(p)}$. In (2.13) and (2.16), $\tilde{q}^{-2}[Z_2-\rho(\tilde{q})]$ corresponds to a Fourier component $V_M(\tilde{q})$ in (2.10) except for a numerical factor.

The quantities $P_{\text{ion}}(\tilde{b})$ and $P_{\text{exc},n}(\tilde{b})$ are rewritten in simple forms:

$$\begin{aligned}&P_{\text{ion}}(\tilde{b})=(Z_2^2/Z_1^2\tilde{v}^2)F_{\text{ion}}(\tilde{b},\tilde{v},\tilde{a}_{\text{TF}}) ,\\ &P_{\text{exc},n}(\tilde{b})=(Z_2^2/Z_1^2\tilde{v}^2)F_{\text{exc},n}(\tilde{b},\tilde{v},\tilde{a}_{\text{TF}}) ,\end{aligned} \tag{2.19}$$

where functions $F_{\text{ion}}(\tilde{b},\tilde{v},\tilde{a}_{\text{TF}})$ and $F_{\text{exc},n}(\tilde{b},\tilde{v},\tilde{a}_{\text{TF}})$ denote the residual parts of $P_{\text{ion}}(\tilde{b})$ and $P_{\text{exc},n}(\tilde{b})$, respectively, except for the leading factor $Z_2^2/Z_1^2\tilde{v}^2$. Such expressions have an important physical meaning in that the ionization and the excitation probabilities in the first-order theory for a hydrogenlike projectile with atomic number Z_2 and velocity v, which collides with an atom with atomic number Z_2 and the screening length a_{TF} at impact parameter b, are identical to those multiplied by a factor Z_2^2/Z_1^2 for a hydrogen atom with the reduced velocity $\tilde{v}$, which collides with a "statistical" hydrogen atom with the reduced screening length $\tilde{a}_{\text{TF}}$ at the reduced impact parameter $\tilde{b}$. In our unitarized impact parameter formalism, the projectile-ionization and -excitation cross sections are obtained by

$$\begin{aligned}&\sigma_{\text{ion}}=Z_1^{-2}\int_0^\infty d\tilde{b}\,2\pi\tilde{b}\,\mathscr{P}_{\text{ion}}(\tilde{b}) ,\\ &\sigma_{\text{exc},n}=Z_1^{-2}\int_0^\infty d\tilde{b}\,2\pi\tilde{b}\,\mathscr{P}_{\text{exc},n}(\tilde{b}) ,\end{aligned} \tag{2.20}$$

where

$$\mathscr{P}_{\rm ion}(\tilde{b})=[P_{\rm ion}(\tilde{b})/P_t(\tilde{b})]\sin^2[P_t(\tilde{b})^{1/2}]\ ,$$
$$\mathscr{P}_{{\rm exc},n}(\tilde{b})=[P_{{\rm exc},n}(\tilde{b})/P_t(\tilde{b})]\sin^2[P_t(\tilde{b})^{1/2}]\ , \qquad (2.21)$$
$$P_t(\tilde{b})=P_{\rm ion}(\tilde{b})+\sum_{n=2}^{\infty}P_{{\rm exc},n}(\tilde{b})\ .$$

If the condition $P_t(\tilde{b})\ll 1$ is satisfied (usually in the case where $\tilde{v}\gg 1$), $\mathscr{P}_{\rm ion}(\tilde{b})$ and $\mathscr{P}_{{\rm exc},n}(\tilde{b})$ can be replaced by $P_{\rm ion}(\tilde{b})$ and $P_{{\rm exc},n}(\tilde{b})$, respectively. Then the ionization cross section $\sigma_{\rm ion}^{\rm el}$ contributed from the target-elastic process is given by

$$\sigma_{\rm ion}^{\rm el}=(Z_2^2/Z_1^4\tilde{v}^2)\tilde{\sigma}_{\rm H}\ ,$$
$$\tilde{\sigma}_{\rm H}=\int_0^\infty d\tilde{b}\,2\pi\tilde{b}F_{\rm ion}(\tilde{b},\tilde{v},\tilde{a}_{\rm TF})\ , \qquad (2.22)$$

where $\sigma_{\rm H}$ denotes the reduced electron loss cross section for a hydrogen atom with velocity $\tilde{v}$ colliding with an atom with $Z_2=1$ and with the screening length $\tilde{a}_{\rm TF}$. When $\tilde{\sigma}_{\rm H}$ depends very weakly on $\tilde{a}_{\rm TF}$, the loss cross-section curves plotted for $(Z_1^4\tilde{v}^2/Z_2^2)\sigma_{\rm ion}$ vs $\tilde{v}$ will be scaled well. The asymptotic forms of the target-elastic contribution $\sigma_{\rm ion}^{\rm el}$ and the target-inelastic one $\sigma_{\rm ion}^{\rm inel}$ for $\tilde{v}\gg 1$ are

$$\sigma_{\rm ion}^{\rm el}\propto Z_2^2/Z_1^4\tilde{v}^2,\quad \sigma_{\rm ion}^{\rm inel}\propto Z_2/Z_1^4\tilde{v}^2\ . \qquad (2.23)$$

The detailed form of $\sigma_{\rm ion}^{\rm inel}$ appears in other papers.[12–14] Either from (2.23) or from the detailed expressions, $\sigma_{\rm ion}^{\rm el}$ is much more dominant than $\sigma_{\rm ion}^{\rm inel}$. It is, therefore, relevant to scale the loss cross section not by $(Z_1^4\tilde{v}^2/Z_2)\sigma$ but by $(Z_1^4\tilde{v}^2/Z_2^2)\sigma$. In our case, to find a scaling on projectile-target combinations, the reduced screening length $\tilde{a}_{\rm TF}$ is considered here. Except for a numerical factor, $\tilde{a}_{\rm TF}$ is determined by $Z_2^{-1/3}Z_1(=c)$. Then we can draw a conclusion that if $\tilde{a}_{\rm TF}$ is kept constant for sets of projectile-target combinations [e.g., $(Z_1,Z_2)=(2,2),(4,16),\ldots$ belong to one set, and $(2,3),(4,24),\ldots$ belong to another set], $P_{\rm ion}(\tilde{b})$ behave like $\sim(Z_2^{4/3}/c^2\tilde{v}^2)F_{\rm ion}(\tilde{b},\tilde{v},c)$ or $\sim(Z_1^4/c^6\tilde{v}^2)F_{\rm ion}(\tilde{b},\tilde{v},c)$, and $P_{{\rm exc},n}(\tilde{b})$, behaves in a way similar to $P_{\rm ion}(\tilde{b})$. Therefore, we obtain

$$\sigma_{\rm ion}^{\rm el}\sim(Z_2^{2/3}/c^4\tilde{v}^2)\int_0^\infty d\tilde{b}\,2\pi\tilde{b}F_{\rm ion}(\tilde{b},\tilde{v},c)$$

or (2.24)

$$\sim(Z_1^2/c^6\tilde{v}^2)\int_0^\infty d\tilde{b}\,2\pi\tilde{b}F_{\rm ion}(\tilde{b},\tilde{v},c)\ .$$

On the other hand, for the case of $P_t(\tilde{b})\gtrsim 1$, $P_{\rm ion}(\tilde{b})$, and $P_{{\rm exc},n}(\tilde{b})$ increase greatly in the small $\tilde{b}$ region, with both quantities exceeding unity. Due to the unitarity, however, it is impossible for $\mathscr{P}_{\rm ion}(\tilde{b})$ and $\mathscr{P}_{{\rm exc},n}(\tilde{b})$ to exceed unity. This fact brings a weaker Z_2 dependence of the loss cross sections than the first-order theory does. This result is attributed to the cancellation of a factor $Z_2^2/Z_1^2\tilde{v}^2$ in the amplitude of $\mathscr{P}_{\rm ion}(\tilde{b})$ and $\mathscr{P}_{{\rm exc},n}(\tilde{b})$, which enters only in the argument of sine functions. If we notice this remarkable feature, we can also expect a weaker Z_1 dependence as well. From (2.20), we can easily realize that the projectile-ionization and -excitation cross sections are scaled as

$$\tilde{\sigma}_{\rm ion}=Z_1^2\sigma_{\rm ion},\quad \tilde{\sigma}_{{\rm exc},n}=Z_1^2\sigma_{{\rm exc},n}\ . \qquad (2.25)$$

It is observed that Z_2 and $\tilde{v}$ do not appear explicitly in (2.25) and are included implicitly in $\tilde{\sigma}_{\rm ion}$ or $\tilde{\sigma}_{{\rm exc},n}$. Since $\tilde{\sigma}_{\rm ion}$ and $\tilde{\sigma}_{{\rm exc},n}$ depend on Z_1 also through $\tilde{a}_{\rm TF}$, we do not expect in general the scaling with respect to Z_1 is simple like (2.25). Nevertheless, the relation $\tilde{\sigma}_{\rm ion}\propto Z_1^m\sigma_{\rm ion}$ $(2.4\le m\le 2.8)$ turns out to be actually valid in the range $\tilde{v}\lesssim 1$ for hydrogenlike projectiles in collisions with several targets treated later.

III. NUMERICAL RESULTS AND DISCUSSIONS

In our previous calculation[16] of the electron-loss cross sections for a He$^+$ ion, the numerical results yield good agreement with the experimental data as a whole. For several targets, however, we found appreciable differences especially in the high impact-velocity region $v\gtrsim 4v_0$. We assume these differences will be caused by the rather crude approximation of $\rho(q)$ in (2.9) to the real form factor. In general, at high impact velocities, the momentum transfer in the z direction (the direction of motion of a projectile), i.e., $\tilde{q}_z$, becomes small, and accordingly, a small momentum transfer ($\tilde{q}$) mainly contributes to the loss cross section. We should, therefore, describe more precisely the form factors there. As a standard of the real form factors, we take the Hartree-Fock form factors. Then our prescription is to modify the parameters in the Molière electron distribution (MED) in order to fit them

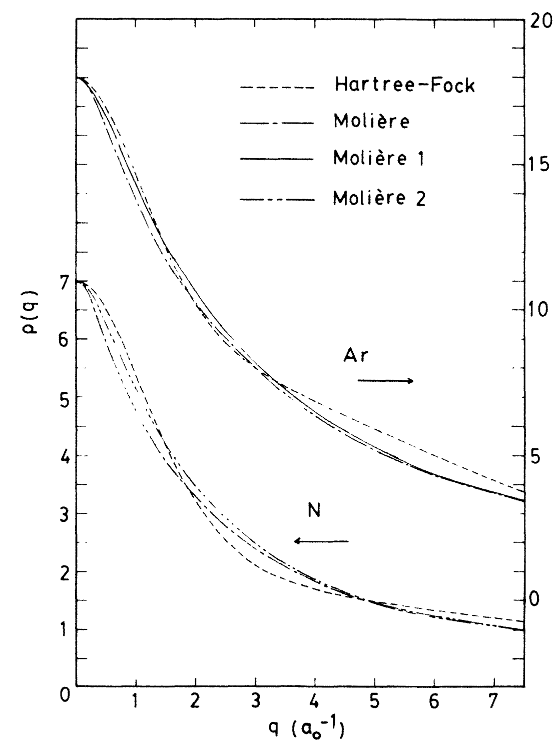

FIG. 1. Form factors of N and Ar atoms calculated from Hartree-Fock (HF) electron distribution (— — —), the Molière electron distribution (MED) (—-—), and the modified MED (—— and —-·-—). The parameters $(\beta_1,\beta_2,\beta_3)$ for the curves denoted by Molière, Molière 1, and Molière 2 are (6.0,1.20,0.30), (6.0,1.20,0.35), and (6.0,1.20,0.40), respectively. The arrows indicate the scale of the vertical axis.

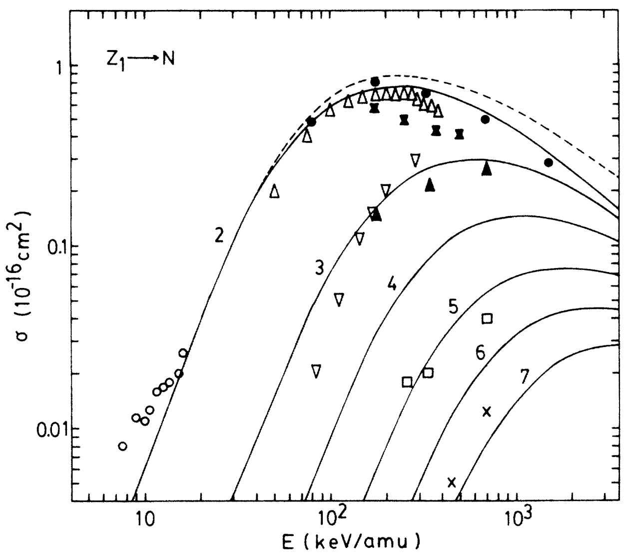

FIG. 2. Electron-loss cross sections for He^+, Li^{2+}, Be^{3+}, B^{4+}, C^{5+}, and N^{6+} ions colliding with a N atom. The dotted line indicates the calculation for a He^+ ion using the Molière electron distribution (MED), and the solid lines indicate those for the above six hydrogenlike ions using the modified MED denoted by Molière 2 in Fig. 1. The numbers near the curves denote the atomic number of the ions. The experimental data are obtained for a He^+ ion (○, Ref. 19; △, Ref. 20; ●, Ref. 21; ⧗, Ref. 22), for a Li^{2+} ion (▲, Ref. 21; ▽, Ref. 23), for a B^{4+} ion (□, Ref. 21), and for a N^{6+} ion (×, Ref. 21).

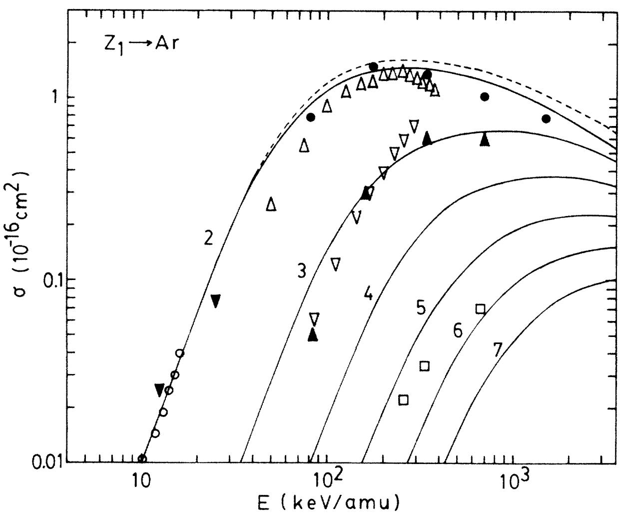

FIG. 3. Electron-loss cross sections for He^+, Li^{2+}, Be^{3+}, B^{4+}, C^{5+}, and N^{6+} ions colliding with an Ar atom. The dotted line indicates the calculation for a He^+ ion using the MED, and solid lines indicate those for the above six hydrogenlike ions using the modified MED denoted by Molière 1 in Fig. 1. The experimental data are same as in Fig. 2 except for a He^+ ion (▼, Ref. 24). The numbers near the curves denote the atomic number of the ions.

especially in a small $\tilde{q}$ region. In Fig. 1 the form factors $\rho(q)$'s are illustrated for N and Ar targets using the Hartree-Fock,[18] the Molière, and the modified Molière electron distributions, where the modified parameters are obtained as $(\beta_1,\beta_2,\beta_3)=(6.0,1.20,0.40)$ for N and (6.0,1.20,0.35) for Ar. The other parameters α_i $(i=1,2,3)$ are not changed in this case. From the figure such modification actually improves $\rho(q)$ in a small q region, while in a large q region no conspicuous differences can be found.

Figures 2 and 3 show the electron-loss cross sections for hydrogenlike projectiles colliding with N and Ar targets, respectively. Calculation was performed for He^+, Li^{2+}, Be^{3+}, B^{4+}, C^{5+}, and N^{6+} ions with specific energy ranging from ~ 10 to 3600 keV/amu. The dotted lines indicate the results from the original Molière form factors of target atoms for a He^+ ion and the solid lines do the results from the modified Molière form factors. Except for a He^+ ion, there are not so many experimental data for other ions. Nevertheless, a comparison of theoretical curves obtained by the modification with data shows good agreement as a whole. In $P_{\rm ion}(\tilde{b})$ and $P_{{\rm exc},n}(\tilde{b})$, the information of targets enters in terms of the charge distribution in the Fourier space, i.e., $Z_2-\rho(\tilde{q})$. In the limit of $\tilde{q}=0$, $Z_2-\rho(\tilde{q})$ is equal to zero since we treat neutral target atoms. Therefore, the improvement of $Z_2-\rho(\tilde{q})$ in a small $\tilde{q}$ region yields a significant influence on the integral over $\tilde{q}_y$ appearing in (2.13) and (2.16). Except for this region, a relative difference in $Z_2-\rho(\tilde{q})$ between the MED and the modified MED is very small since $Z_2-\rho(\tilde{q})$ itself is considerably large. Moreover at high and low impact velocities, small and large $\tilde{q}_z$ values in (2.14) dominantly contribute to the loss cross section. Judging from the above consideration, the modified MED improves greatly the loss cross section at high velocities, while it has almost no affect at low velocities.

In Figs. 4–7 the calculated electron loss cross sections for He^+, Li^{2+}, Be^{3+}, B^{4+}, C^{5+}, and N^{6+} ions with the reduced velocity $\tilde{v}$ ranging from $\sim 0.3v_0$ to $6v_0$ in collisions with N, O, Ne, and Ar targets are shown together with the reported data.[19–24] The modified MED's for O and Ne are described by $(\beta_1,\beta_2,\beta_3)=(6.0,1.20,0.50)$ and (6.0,1.20,0.60), respectively. Here we have expressed the scaled cross section $\tilde{\sigma}_{\rm ion}$ in the form of $\tilde{\sigma}_{\rm ion}=Z_1^m\sigma_{\rm ion}$ as a function of the reduced velocity $\tilde{v}=v/Z_1$. Then we obtain $m=2.8$ for N and O, 2.6 for Ne, and 2.4 for Ar. These power indices are determined by considering the cross sections in the lower reduced velocity range $\tilde{v}\lesssim 1$. With increasing Z_2 number, the Z_1 dependence of the scale factor of $\tilde{\sigma}_{\rm ion}$ becomes weak. At a glance we can easily notice that the reduced peak velocities $\tilde{v}_p$'s at which $\tilde{\sigma}_{\rm ion}$'s get maximum for the above ions $(2\leq Z_1\leq 7)$ are located at about 2 not at 1. The latter reduced velocity, i.e., $\tilde{v}=1$, corresponds to $\tilde{v}_p$ predicted from the FBA theory. In addition, $\tilde{v}_p$ value is shifted a bit toward the higher velocity side with increasing Z_1. As far as the velocity dependence is concerned, the (reduced) loss cross sections behaves like $\tilde{v}^{5.6}$ in the range of $0.3v_0\lesssim\tilde{v}\lesssim v_0$, and also

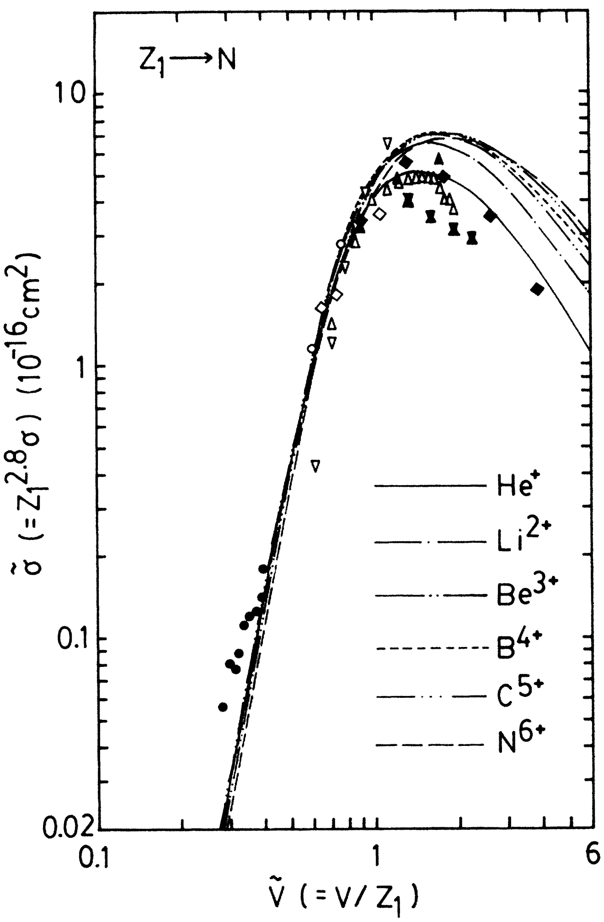

FIG. 4. The scaled loss cross section $\tilde{\sigma}$ $(=Z_1^{2.8}\sigma)$ vs $\tilde{v}$ $(=v/Z_1)$ for He^+, Li^{2+}, Be^{3+}, B^{4+}, C^{5+}, and N^{6+} ions colliding with a N target. The experimental data are obtained for a He^+ ion (●, Ref. 19; △, Ref. 20; ♦, Ref. 21; ⧗, Ref. 22), for a Li^{2+} ion (▲, Ref. 21; ▽, Ref. 23), for a B^{4+} ion (◇, Ref. 21), and for a N^{6+} ion (○, Ref. 21).

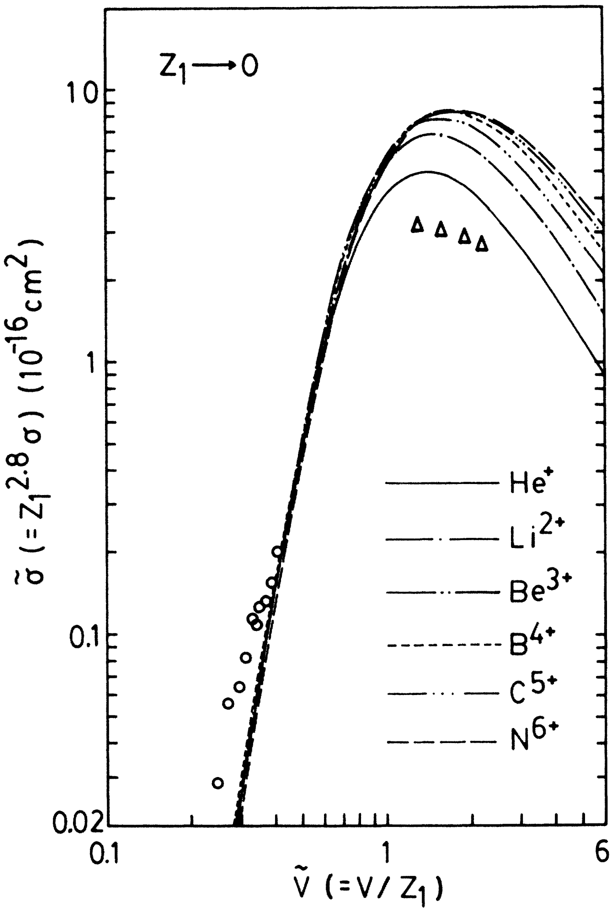

FIG. 5. The scaled loss cross section $\tilde{\sigma}$ $(=Z_1^{2.8}\sigma)$ vs $\tilde{v}$ $(=v/Z_1)$ for He^+, Li^{2+}, Be^{3+}, B^{4+}, C^{5+}, and N^{6+} ions colliding with an O target. The experimental data are obtained for a He^+ ion (○, Ref. 19; △, Ref. 22).

nearly $\tilde{v}^{-1}$ for $2v_0 \lesssim \tilde{v} \lesssim 6v_0$. The latter rough estimate is consistent with Bohr formula. At much higher velocities, one can naturally expect that the loss cross sections have approximately a dependence of $\tilde{v}^{-2}$ from the theoretical point of view, since the first-order theories are applicable. Compared with the FBA, another feature is that in our theory the loss cross sections have broader peaks as a function of velocity. This is due to the reduction of the loss cross section around the peak velocity predicted from the first-order theory by means of estimating the higher-order interaction terms as well as the first one. Our evaluation method of higher-order matrix elements is interpreted as a modification of the existence probability of the initial state.[16] This modification was made by introducing excitation channels as well as ionization channels into the formalism. In our scheme, the residual part of transition probability except for the oscillating factor means the relative transition probability for a given reaction to the total transition probability for all reactions in the framework of Born approximation at each impact parameter. Then the bound electron in the initial state is also allowed to be excited in the discrete states. The present treatment is necessary for the reduced velocity range $\tilde{v} \lesssim 1$. In much higher velocity ranges, the excitation probabilities can be neglected in comparison with the ionization one because there the FBA can be applied successfully. We should note here that the relativistic effect is not included in our calculation.

An important effect of highly charged projectiles on target atoms is to polarize the electron cloud, which has not been taken into account in the paper. Qualitatively, this polarization effect decreases the electric potential field set up by a target atom so that the projectile encounters a slightly weakened effective potential field. In this sense, our theoretical estimate of the loss cross sections for highly charged projectiles would have to give smaller values especially at low impact velocities. A quantitative treatment of the polarization, however, is a future task of ours.

In summary, on the basis of the previously presented method, we have studied the projectile-ionization cross sections for hydrogenlike ions with atomic number rang-

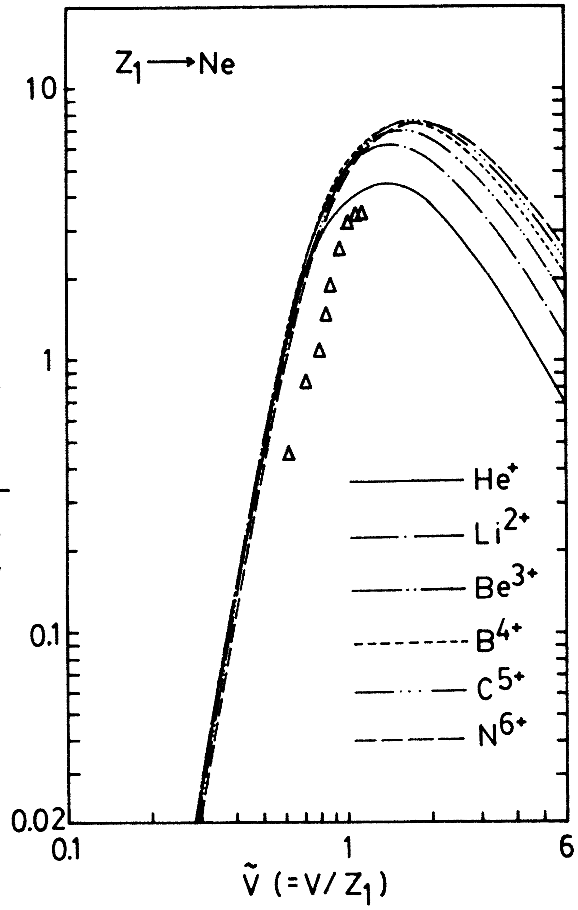

FIG. 6. The scaled loss cross section $\tilde{\sigma}$ $(=Z_1^{2.6}\sigma)$ vs $\tilde{v}$ $(=v/Z_1)$ for He^+, Li^{2+}, Be^{3+}, B^{4+}, C^{5+}, and N^{6+} ions colliding with a Ne target. The experimental data are obtained for a Li^{2+} ion ($\triangle$, Ref. 23).

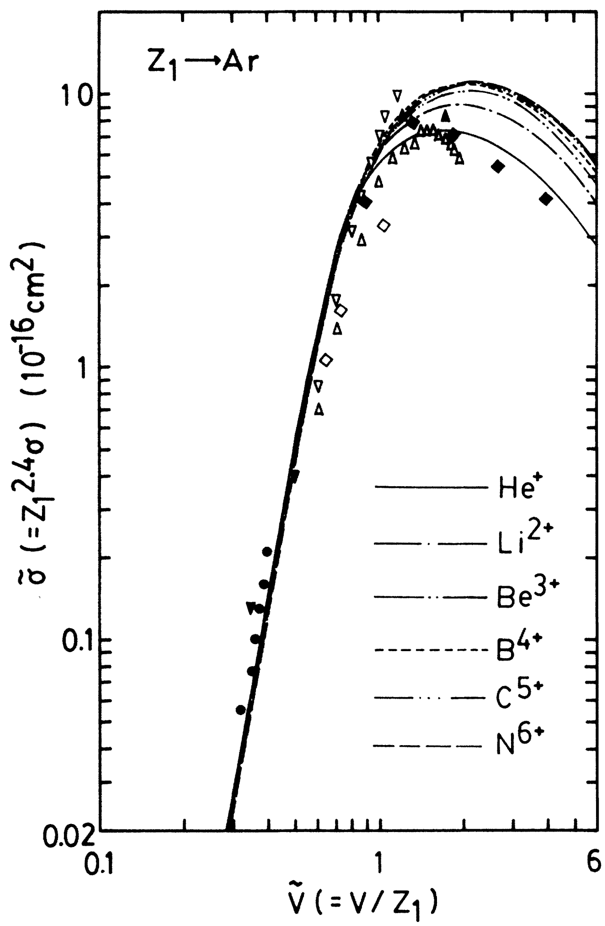

FIG. 7. The scaled loss cross section $\tilde{\sigma}$ $(=Z_1^{2.4}\sigma)$ vs $\tilde{v}$ $(=v/Z_1)$ for He^+, Li^{2+}, Be^{3+}, B^{4+}, C^{5+}, and N^{6+} ions colliding with an Ar target. The experimental data are same as in Fig. 4 except for a He^+ ion ($\blacktriangledown$, Ref. 24).

ing from 2 to 7 and with the reduced velocity ranging from $0.3v_0$ to $6v_0$ in collisions with N, O, Ne, and Ar targets. One could see the importance of the atomic form factors in the small momentum-transfer region in estimating the loss cross sections at high velocities. Neglecting the polarization of target atoms, the loss cross sections can be well scaled especially at lower velocities than the peak velocity. We presented the scale factor Z_1^m in the relation $\tilde{\sigma}_{\text{ion}}=Z_1^m\sigma_{\text{ion}}$, where $m=2.8$ for N and O, 2.6 for Ne, and 2.4 for Ar. Formally, $m=2$ is straightforwardly obtained as appeared in (2.25). These scale factors are different from Z_1^4, which the first Born approximation predicts. Finally, we eagerly expect much more experimental data, which covers a wide velocity (or energy) range of hydrogenlike ions, will be reported in the future to help in the further development of the theory.

ACKNOWLEDGMENTS

The author would like to express his sincere thanks to Professor Y. Yamamura of Okayama University of Science and Professor Y. H. Ohtsuki of Waseda University for their useful discussions. This work was sponsored by a Grant-in-Aid for Fundamental Scientific Research from the Ministry of Education, Japan.

[1]H. A. Bethe, Ann. Phys. (Leipzig) **5**, 325 (1930).
[2]F. Bloch, Ann. Phys. (Leipzig) **16**, 285 (1933).
[3]J. Lindhard and A. Winther, K. Dan. Vidensk. Selsk. Mat. Fys. Medd. **34**, No. 4 (1964).
[4]N. Bohr, K. Dan. Vidensk. Selsk. Mat. Fys. Medd. **18**, No. 8 (1948).
[5]J. Lindhard and M. Scharff, K. Dan. Vidensk. Selsk. Mat. Fys. Medd. **27**, No. 15 (1953).
[6]As books of compiled data, J. F. Ziegler, in *The Stopping and Ranges of Ions in Matter*, edited by J. F. Ziegler (Pergamon, New York, 1977, 1980), Vols. 2–6.
[7]T. L. Ferrell and R. H. Ritchie, Phys. Rev. B **16**, 115 (1977).
[8]W. Brandt and M. Kitagawa, Phys. Rev. B **25**, 5631 (1982).
[9]T. Kaneko, Phys. Rev. A **30**, 1714 (1984); 33, 1602 (1986).

[10]T. Kaneko and Y. Yamamura, Phys. Rev. A **33**, 1653 (1986); Nucl. Instrum. Methods Phys. Res. **B13**, 119 (1986).

[11]H.-D. Betz, Rev. Mod. Phys. **44**, 465 (1977); *Methods of Experimental Physics* (Academic, New York, 1980), Vol. 17, p. 73.

[12]G. H. Gillespie, Phys. Rev. A **18**, 1967 (1978).

[13]D. W. Rule, Phys. Rev. A **16**, 19 (1977).

[14]I. S. Dmitriev, Ya. M. Zhileikin, and V. S. Nikolaev, Zh. Eksp. Teor. Fiz. **49**, 500 (1965) [Sov. Phys.—JETP **22**, 352 (1966)].

[15]See Chap. 4. of Ref. 4.

[16]T. Kaneko, Phys. Rev. A **32**, 2175 (1985).

[17]It should be noted that approximations (1) and (2) in the text were first adopted in the successful study of the electron-transfer problem by H. Ryufuku and T. Watanabe (RW) [Phys. Rev. A **19**, 1538 (1979)], where they treated a pure three-body problem and the state vector of the transferred electron was expanded in terms of "traveling eigenstates." Their method is called the "unitarized distorted-wave approximation (UDWA)." In our case, the state vector is expanded in terms of the products of eigenstates belonging to two independent systems, and only the excitation process, including ionization and excluding electron capture, have been treated. When we study the excitation of collision partners composed of a point charge and a particle with one electron, (2.2) in the text is immediately included in (2.28) of RW, which is expected to yield more accurate results because of the consideration of the capture process. In this sense, our method is not quite different from UDWA. If we neglect the differences in electron capture or excitation, traveling eigenstates or products of eigenstates of independent two systems, and three-body (one electron and two nuclei) problems or many-body (more than two electrons and two nuclei) problems, the formula (2.2) would correspond to (2.28) of RW. We consider target atoms with Z_2 (≥ 2) electrons and neglect the distortion. The total probability is conserved in our study. On this basis, we call our method the "unitarized impact-parameter method."

[18]E. Clementi and C. Roetti, At. Data Nucl. Data Tables **14**, 177 (1974).

[19]M. B. Shah and H. B. Gilbody, J. Phys. B **8**, 372 (1975).

[20]L. I. Pivovar, V. M. Tubaev, and M. T. Novikov, Zh. Eksp. Teor. Fiz. **41**, 26 (1961) [Sov. Phys.—JETP **14**, 20 (1962)].

[21]I. S. Dmitriev, V. S. Nikolaev, L. N. Fateeva, and Ya. A. Teplova, Zh. Eksp. Teor. Fiz. **42**, 16 (1962) [Sov. Phys.—JETP **15**, 11 (1962)].

[22]A. Itoh, K. Ohnishi, and F. Fukuzawa, J. Phys. Soc. Jpn. **49**, 1513 (1980).

[23]L. I. Pivovar, Yu. Z. Levchenko, and G. A. Krivonosov, Zh. Eksp. Teor. Fiz. **59**, 19 (1970) [Sov. Phys.—JETP **32**, 11 (1971)].

[24]P. R. Jones, F. P. Ziemba, H. A. Moses, and E. Everhart, Phys. Rev. **113**, 182 (1959).